Annals of Botany **108**: 991–1000, 2011
doi:10.1093/aob/mcr064, available online at www.aob.oxfordjournals.org

ANNALS OF BOTANY
Founded 1887

PART OF A SPECIAL ISSUE ON FUNCTIONAL–STRUCTURAL PLANT MODELLING

Reconstruction and analysis of a deciduous sapling using digital photographs or terrestrial-LiDAR technology

Sylvain Delagrange[1,2,*] and Pascal Rochon[1]

[1]*University of Quebec in Outaouais (UQO) – IQAFF, 58 Main Street, Ripon, QC, J0V 1V0, Canada and* [2]*Centre for Forest Research (CFR) UQAM, PO Box 8888, Centre-Ville Station, Montreal, Quebec, Canada H3C 3P8*
** For correspondence. E-mail sylvain.delagrange@uqo.ca*

Received: 3 December 2010 Returned for revision: 7 January 2011 Accepted: 10 February 2011 Published electronically: 22 April 2011

• *Background and Aims* To meet the increasing need for rapid and non-destructive extraction of canopy traits, two methods were used and compared with regard to their accuracy in estimatating 2-D and 3-D parameters of a hybrid poplar sapling.
• *Methods* The first method consisted of the analysis of high definition photographs in *Tree Analyser* (TA) software (PIAF-INRA/Kasetsart University). TA allowed the extraction of individual traits using a space carving approach. The second method utilized 3-D point clouds acquired from terrestrial light detection and ranging (T-LiDAR) scans. T-LiDAR scans were performed on trees without leaves to reconstruct the lignified structure of the sapling. From this skeleton, foliage was added using simple modelling rules extrapolated from field measurements. Validation of the estimated dimension and the accuracy of reconstruction was then achieved by comparison with an empirical data set.
• *Key Results* TA was found to be slightly less precise than T-LiDAR for estimating tree height, canopy height and mean canopy diameter, but for 2-D traits both methods were, however, fully satisfactory. TA tended to over-estimate total leaf area (error up to 50 %), but better estimates were obtained by reducing the size of the voxels used for calculations. In contrast, T-LiDAR estimated total leaf area with an error of <6 %. Finally, both methods led to an over-estimation of canopy volume. With respect to this trait, T-LiDAR (14·5 % deviation) greatly surpassed the accuracy of TA (up to 50 % deviation), even if the voxels used were reduced in size.
• *Conclusions* Taking into account their magnitude of data acquisition and analysis and their accuracy in trait estimations, both methods showed contrasting potential future uses. Specifically, T-LiDAR is a particularly promising tool for investigating the development of large perennial plants, by itself or in association with plant modelling.

Key words: T-LiDAR, *Tree Analyser* software, 2-D and 3-D trait extraction, hybrid poplar, crown reconstruction, digital photographs.

INTRODUCTION

Over the past two decades, numerous studies have been conducted to develop rapid and non-destructive methods of extracting individual tree characteristics. Such information is crucial to both forest practitioners and private land owners for monitoring tree growth and stem quality in plantation systems or in natural forests where a silvicultural system is based on selective cutting. Furthermore, these tree characteristics must be measured with some accuracy to feed models that predict regeneration processes, dynamics and yield at the individual (Perttunen *et al.*, 2001; Lambert *et al.*, 2005; Houllier and de Reffye, 2006) or stand level (Pacala *et al.*, 1993; Doyon *et al.*, 2006).

Realistic reconstruction of individual trees has been explored using digitizing devices (Sinoquet *et al.*, 1998; Farque *et al.*, 2001; Di Iorio *et al.*, 2005; Delagrange *et al.*, 2006). This technique has the advantage of precisely locating the positions of tree elements (i.e. leaves, petioles, segments and branching points) and providing their orientations in a 3-D space. Although the coupling of partial tree digitizing and simplified reconstruction is possible (Sonohat *et al.*, 2006), the time and logistic requirements needed for field data acquisition are considerable. This usually constrains the digitizing method to small-statured individuals and to more theoretical questions such as biotic and abiotic variability of crown light interception efficiency (Delagrange *et al.*, 2006; Chambelland *et al.*, 2008). Consequently, methods that would allow rapid and greater operational field data acquisition (i.e. remote sensing) combined with post-treatment analyses may represent the best avenue for routine extraction of tree traits.

In the last decade, two main approaches have been developed regarding remote sensing at the individual tree level. First, tree and crown dimensions can be estimated from one or several digital photographs (Shlyakhter *et al.*, 2001; Mizoue and Masutani, 2003; Phattaralerphong and Sinoquet, 2005; Tan *et al.*, 2008). Phattaralerphong and Sinoquet (2007) developed Tree Analyser (TA), which is free software based on this approach. Several viewpoints are generally needed to extract 3-D traits from digital photographs, with subsequent estimation of tree volume based on a space carving procedure (Martin and Aggarwal, 1983; Phattaralerphong and Sinoquet, 2005). Under natural conditions, such as those

encountered in the forest understorey, this method faces critical limitations associated with the lack of contrast between the target tree and its background (Mizoue and Masutani, 2003). Neubert *et al.* (2007) and Tan *et al.* (2008) also developed methods to reconstruct 3-D crowns from only one picture, but these techniques were aimed at generating realistic-looking trees for movie post-production, architectural designs and games, rather than remote sensing applications for foresters.

The second promising approach uses T-LiDAR (terrestrial light detection and ranging) to make high resolution laser scans of vegetation (Hosoi and Omasa, 2006; Xu *et al.*, 2007; Bucksch *et al.*, 2009; Côté *et al.*, 2009; Rosell *et al.*, 2009; Yan *et al.* 2009; Preuksakarn *et al.*, 2010). Extremely efficient in locating objects in 3-D space, this approach can assess the complexity of crown organization, but the development of robust algorithms making full use of the information is generally long and complex (e.g. Côté, 2010; Preuksakarn *et al.*, 2010). Since this approach aims to reconstruct all elements of the tree, rather than just shapes and volumes, occlusion might therefore become more detrimental for accurate data acquisition.

One additional benefit of crown reconstruction via remote sensing methods is that the reconstructed individual includes the imprint left on the tree shape by all past stochastic events (Pearcy *et al.*, 2005). As a consequence, the extracted information is expected to mirror reality very closely and it may represent an invaluable portrait of an individual's structure at a given point in time. Such information can be used (*a*) as an accurate database for the validation (which is generally difficult to achieve) of long-term simulations using a functional–structural plant model (FSPM) or (*b*) as input to those FSPM modelling exercises.

The reconstruction of individual trees from photographs or T-LiDAR scans is independent of phyllotaxic or architectural rules, making these methods easily adaptable to multiple species (Phattaralerphong and Sinoquet, 2005; Côté *et al.*, 2009). Furthermore, through the use of L-System grammar (cf. Prusinkiewicz *et al.*, 2007), bridges between remote sensing and modelling have already been tested and have increased the quality of large tree reconstructions (Côté *et al.*, 2009). Nevertheless, several limitations must first be addressed to allow a broader use of remote sensing and reconstruction of *in situ* trees. In particular, the T-LiDAR approach needs the development of algorithms specific to individual species and sizes. These methods also require robust validation against empirical data, which are usually difficult to obtain. Here, we proposed to test two methods based on two remote sensing approaches (i.e. digital photographs and T-LiDAR scans) for individual tree reconstructions and to apply them to a deciduous species and in an operational context. More specifically, we aimed at identifying a method providing (*a*) rapid and accurate extraction of traits, thereby allowing the estimation of growth yields and stem quality of planted trees, and (*b*) a spatially explicit reconstruction of leaf area which may be used to model growth and yields of these planted trees.

The three specific objectives of the study were thus: (1) to reconstruct the form and volume of a deciduous sapling crown from either T-LiDAR scans (after developing simple and robust algorithms and allometric relationships) or digital photographs after parameterizing the TA software (Phattaralerphong and Sinoquet, 2007); (2) to extract, from both reconstructions, some 2-D and 3-D parameters of the sapling and compare these with empirical measurements; and (3) to evaluate and discuss future uses for these methods and the opportunities to link them to FSPM.

MATERIALS AND METHODS

Plant material and growing conditions

The plant used to test both methods of virtual reconstructions was a hybrid poplar clone (3230) widely used in plantation systems for afforestation in southern Québec. Planted in June 2008 in a 20 L pot, this sapling originated from a clone cutting of *Populus trichocarpa* Torr. & A.Gray (Section Tacamahaca) × *P. deltoides* W.Bartram ex Marshall (Section Aigeiros) and was grown in a nursery for 2 years. The soil mixture in the pot was composed of sand (1/3 by volume) and forest peat (2/3 by volume). Fertilization was performed in July 2008 and in June 2009 using 100 mL of controlled-release fertilizer (Smartcote, Feed and Forget, 14-14-14 NPK, Spectrum Brands IP Inc., Brantford, ON, Canada). Watering was provided by an automatic system (Shrubber Drip Adjustable Flow System, Anteclo, Longwood, FL, USA) which supplied water to bring the soil to field capacity (i.e. about 5 L) every 3 d.

Reconstruction from digital images

In September 2009, the hybrid poplar sapling was returned to the greenhouse for digital photographs, which were taken from three sides. The three digital photographs were obtained in such a manner as to allow the image processing software to classify picture elements as vegetation or background, i.e. to dichotomize ('binarize') the image into black and white (cf. Fig. 1A). Photographic documentation included camera focal length, camera angles (elevation and azimuth), camera horizontal distance from the sapling and camera height (Phattaralerphong and Sinoquet, 2007). The black and white digital images were loaded into TA software v1.20 to extract tree and crown heights, crown volume and total leaf area (Phattaralerphong and Sinoquet, 2007). Briefly, TA first defines extreme lateral and vertical points of the crown for each viewpoint to compute distances. Secondly, the software creates a volume containing the whole crown and divides this volume into a regular grid in 3-D space. In doing so, the software produces a set of cubic bounding boxes or voxels. Thirdly, the number of voxels is iteratively narrowed using the information contained in each digital photograph (see a detailed description of the methods in Phattaralerphong and Sinoquet, 2005). The size of bounding boxes is user defined. While smaller voxel sizes increase precision (Fig. 1B, C), they also dramatically increase the running time of calculation. Finally, the user has to provide mean leaf area (A_l mean, cm^2) and mean leaf elevation angle (θ_l mean, $^\circ$) to compute total leaf area from the calculated crown volume (Phattaralerphong and Sinoquet, 2007). Here, no distinction is made between voxels containing stem or foliage, assuming that stem represents a small proportion of the whole crown volume. Mean A_l and mean θ_l were measured on a sub-sample of 30 leaves randomly selected within the sapling crown. A list

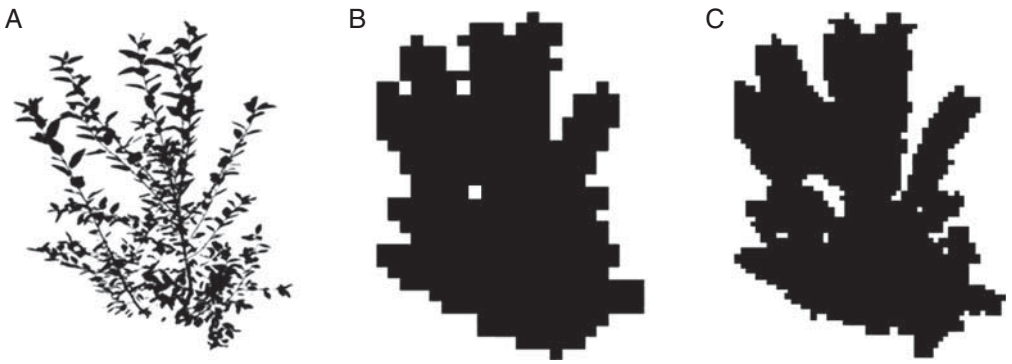

FIG. 1. Illustrations of the studied poplar sapling from the horizontal. Black and white digital picture of the crown after image processing (A), the crown volume as extracted from TA (Tree Analyser) using voxel sizes of 7 cm (B), or 3 cm (C).

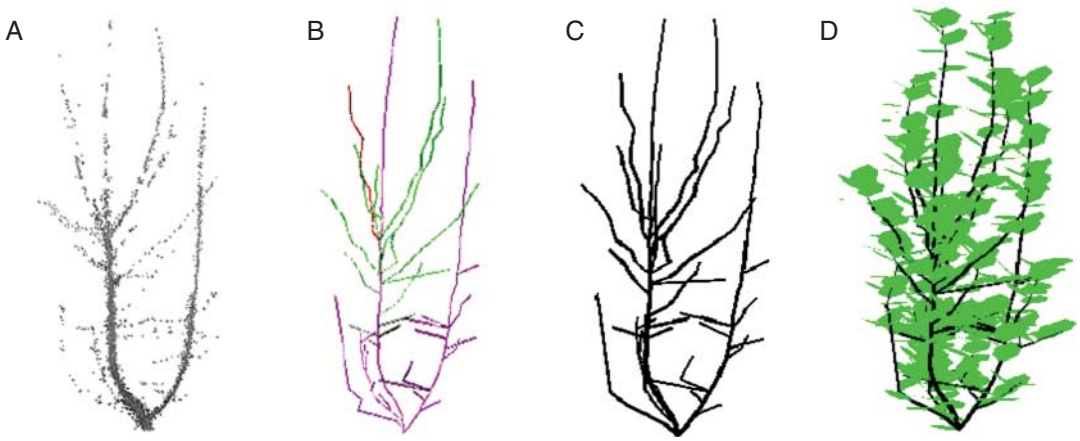

FIG. 2. Main steps of crown reconstruction from T-LiDAR scans. (A) Registered point cloud of the leaf-off scene (B), reconstructed skeleton, (C) pipe representation with reconstructed radius (D) and positioned leaves on the reconstructed pipe representation.

of parameters and abbreviations used throughout the text is given in the Appendix.

Reconstruction from terrestrial LiDAR scans

Following the photography shoot, the hybrid poplar sapling was scanned in a large open area. The scanned scene consisted of the hybrid poplar sapling and four simple geometric objects arranged at 1 m distances around the sapling. A first set of four scans (each at a distance of about 12 m) was performed around the sapling (leaf-on scene) that was only used for validation (see the 'Empirical measurements of targeted traits for validation' section below). Then, all leaves were carefully harvested to measure total leaf area, and a second set of four scans (leaf-off scene) was performed (at a similar distance to the target) for sapling reconstruction. Scans were made using a T-LiDAR device (Ilris-3D, Optech Inc., Vaughan, ON, Canada) that operates at 1500 nm, and which scans with a maximum field-of-view window of 40º × 40º. Beam divergence is 0·00974º (leading to a 14 mm beam footprint at 12 m) and the minimum spacing between two beams is 0·00115º. For these scan exercises, only the last pulse was recorded to allow better sampling of small objects deeper in the crown.

Scan post-treatment started with the filtering and registration of point clouds using 3DImageSuite software (PointStream Inc., Mississauga, ON, Canada). The first filtering removed all points beyond a 2 m radius circle centred on the sapling base. The registration procedure for multiple points of view was performed iteratively to reconstruct the whole 3-D point cloud scene. To do this, three references (i.e. simple geometrical objects arranged around the sapling) were used to define 'matching points'. Then, in a second step, a logical registration procedure merged both sets of points into one co-registered point cloud. Finally, the point cloud representing the sapling was isolated and all other points were removed from the 3-D registered scene (Fig. 2A).

From the leaf-off scene, 210 layers (1-cm widths) were extracted along the vertical z-axis and were analysed using Python-based programming within ArcGIS libraries (ESRI Canada Ltd, Toronto, ON, Canada). For each horizontal layer, groups of points were defined, based on their distance to neighbours. Do to this, a 1 cm radius area was centred on each point ('buffer' tool, ESRI Canada Ltd), thereby generating surfaces composed of overlapping disks. For each layer, the number of groups was thus equivalent to the number of union surfaces created ('dissolve' and 'multi-to-single-part' tools, ESRI Canada Ltd). For each union surface, a centroid was produced ('calculate-field' tool with centroid option,

ESRI Canada Ltd) and categorized with two parameters (i, the layer number and, j, the centroid number in layer i). Then, to link centroids, a simple bottom-up construction rule based on a minimum spanning tree calculation was set using i, and centroid distances between one another. These linkage steps permitted the reconstruction of a skeleton, which was built with a series of line segments (Fig. 2B). Skeleton reconstruction terminated with assignment of a diameter to each line segment, thereby creating a realistic pipe representation (Fig. 2C). At each centroid j of layer i, this diameter corresponded to twice the mean distance ($D_{i,\ j,\mathrm{mean}}$) of the distances from the centroid to the edges of its union surface.

The final step in sapling reconstruction was the addition of foliage. To keep it simple, this canopy reconstruction was based on four very simple but strong rules as follows. (1) Each leaf is attached at points equidistant from others on the current-year shoot only. In other words, leaves only appear along each axis from its tip to the first ramification. (2) On each shoot, the number of leaves (N_l) and maximal leaf length ($L_\mathrm{l,max}$) depend on the current-year length of the shoot (L_s; Fig. 3A, B):

$$N_\mathrm{l} = 0{\cdot}19L_\mathrm{s} + 5{\cdot}44 \quad (1)$$

$$L_\mathrm{l,max} = 4{\cdot}08L_\mathrm{s}^{0{\cdot}32} \quad (2)$$

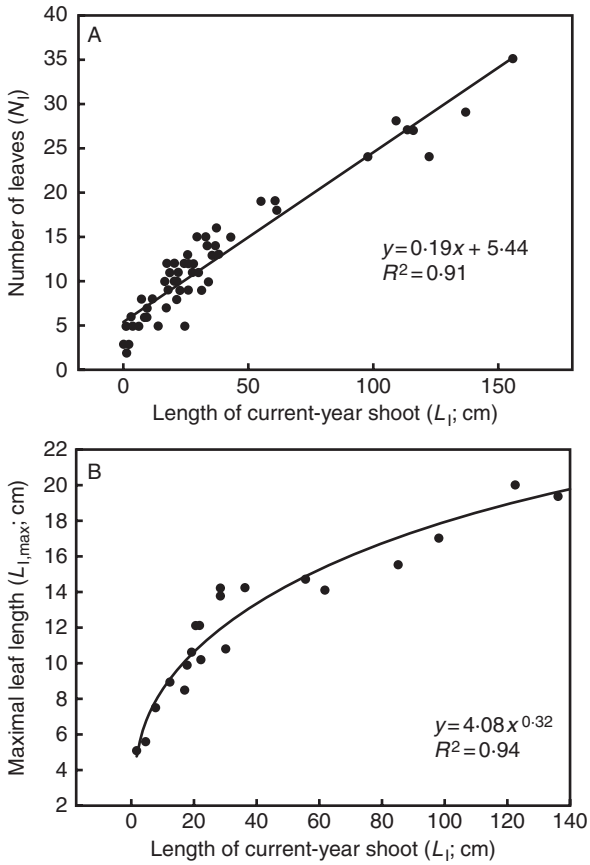

FIG. 3. Allometric relationships used for foliage reconstruction. (A) Relationships between the number of leaves (N_l) and the length of the current-year shoot (L_s), and (B) relationships between the maximal leaf length ($L_\mathrm{l,max}$) and the length of the current-year shoot (L_s).

(3) As defined by field measurements, the area of a leaf (A_l) is dependent on lamina length [L_l; eqn (3), Fig. 4], which is a fraction (β) of the maximal leaf length ($L_\mathrm{l,max}$) according to the relative position of the leaves on the shoot [$L_\mathrm{rel.pos.}$; eqn (4)].

$$A_\mathrm{l} = 0{\cdot}66L_\mathrm{l}^{1{\cdot}80} \quad (3)$$

$$L_\mathrm{l} = \beta L_\mathrm{l,max} \quad (4)$$

where β is a coefficient that varies between 0 and 1 and which follows these linear equations:

$$\beta = 0{\cdot}98L_\mathrm{rel.pos.} + 0{\cdot}36 \quad (5a)$$

when $0 < L_\mathrm{rel.pos.} < 0{\cdot}653$

$$\beta = -0{\cdot}82L_\mathrm{rel.pos.} + 1{\cdot}53 \quad (5b)$$

when $0{\cdot}654 < L_\mathrm{rel.pos.} < 1$

(4) Leaf angles (rolling, Φ_l; elevation, θ_l; and azimuth, Ψ_l) are set as sets of random values between −5 and 5° for Φ_l, between 0 and 45° for θ_l, and between −20 and 20°, iteratively shifted by $+120^\circ$ for each successive leaf on each axis for Ψ_l.

These relationships were determined on an independent set ($n = 10$; 1–2 branches sampled per sapling) of saplings that were the same age and from the same clone as the test subject.

Trait extraction from the reconstructed crown

Six traits were estimated using both reconstruction methods. Tree height (H_t, cm), tree length along the main axis (L_t, cm), crown height (H_c, cm) and mean crown diameter in four horizontal directions (D_c mean, cm) corresponded to the 2-D traits, while total leaf area of the crown (A_c, cm^2) and crown volume (V_c, m^3) related to 3-D traits. The 2-D trait extraction from T-LiDAR scans was rapidly achieved using the pipe representation (Fig. 2C) by searching for extreme values in the point coordinates on the z-axis (for H_t) and in the respective horizontal directions (for $D_\mathrm{c,mean}$). H_c was retrieved using the lower z-co-ordinate for the first segment of the first living

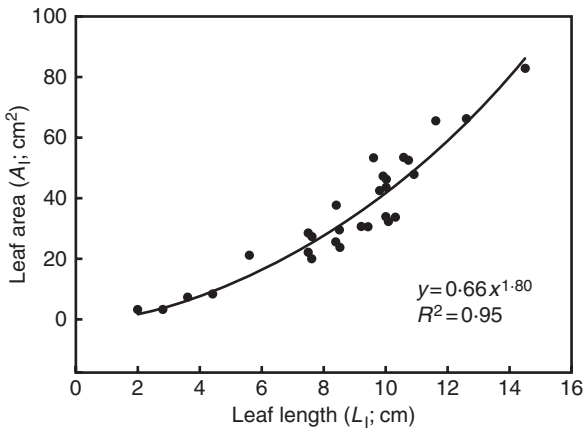

FIG. 4. Allometric relationships between leaf area (A_l) and leaf length (L_l) used for foliage reconstruction.

branch, and the upper z-value among all co-ordinates. L_t was calculated as the length of all segments of the main stem in the pipe representation (Fig. 2C). A_c was computed after the addition of foliage (Fig. 2D) by summing the area of each reconstructed leaf. Finally, V_c was calculated as the sum of the cylinders that fitted on each shoot. The volume of each cylinder was obtained by using the L_b (branch length) and $L_{l,max}$ (maximal leaf length) of each branch as the cylinder length and radius, respectively.

After crown reconstruction with TA, the 2-D and 3-D traits were extracted with two levels of precision (i.e. two sizes of voxels). Reducing the size of voxels greatly increased the definition of the reconstruction (cf. Fig. 1B, C) but also exponentially increased the number of elements that need to be analysed and, therefore, the calculation time. Here, we used 7 and 3 cm for voxelization (hereafter referred to as TA-7 and TA-3, respectively), meaning that for each of the three viewpoints, about 900 and 4900 voxels were analysed, respectively. After parameterization, extraction of all six traits on a standard desktop computer took about 2 and 6 h for 7 and 3 cm voxels, respectively. In TA, L_t cannot be estimated because TA algorithms were not set to isolate and analyse the stem independently. Thus, no distinction in TA is made between H_t and L_t, which are given the same value.

Empirical measurements of targeted traits for validation

To validate the quality of trait extractions for both methods, empirical measurements were made directly on the studied sapling. H_t was defined as the vertical distance between tree base and tree top. L_t corresponded to the distance from tree base to tree top along the main stem. H_c was defined as the vertical distance between the height of the first living branch insertion point on the main stem and the top of the tree. $D_{c,mean}$ averaged the horizontal width of the crown in four marked directions. V_c was the most difficult trait to acquire for validation. However, crown volume was assessed using the registered point clouds of the leaf-on scene obtained from T-LiDAR scans. From this scene (treated with the same filtering and registration as the leaf-off scene, cf. the 'Reconstruction from terrestrial LiDAR scans' section), 1 cm wide layers were extracted and each point was transformed into a 1 cm^2 surface ('buffer' tool, ESRI Canada Ltd). For each layer, a union surface was then calculated ('dissolve' and 'multi-to-single-part' tools, ESRI Canada Ltd) and the volume was then calculated as the integration of all layer surfaces on the z-axis. Finally, total leaf area was measured after all leaves were harvested with a portable leaf area meter (Li-3000A, Li-COR Inc., Lincoln, NE, USA).

In a second step, to test the accuracy of sapling reconstruction from T-LiDAR further, another batch of traits was selected to validate the reconstruction of finer and more isolated elements. To do so, the height of insertion on the main stem (H_b; m) and the length (L_b; m, defined as the distance along the branch from the main stem insertion point to the branch tip) were measured for each branch, and compared with reconstructed branches. Finally, using the volume estimate from the leaf-on scene, a vertical profile of biomass was produced and compared with the vertical distribution of reconstructed objects of the whole sapling.

Visualization

Visualization of crown volumes that were obtained with TA (Fig. 1B, C), together with the reconstructed skeleton (Fig. 2B), pipe structure (Fig. 2C) and whole sapling (Fig. 2D) obtained from T-LiDAR scans, was achieved using VegeSTAR v3.2.4 (Adam *et al.*, 2006). For both methods, visualization allowed us to check the concordance between the virtual reconstruction and the actual structure.

Statistical analysis

All data analyses were performed in an effort to compare and validate trait estimations from reconstructed crowns as compared with actual measured values. First, they consisted of computing deviations in extracted dimensions as compared with measured values. These deviations were expressed as a percentage to be easily comparable. In a second step, the absolute error of estimated traits was calculated to obtain a value with corresponding units for these deviations. Finally, to compare the distribution of biomass along a vertical profile of the crown, normalized biomass was calculated for (*a*) the reconstructed crown from T-LiDAR scans and (*b*) the estimated volume from the registered leaf-on scene. To help in the comparison, the normalized deviation between reconstructed and actual vertical distributions was calculated along the vertical profile.

RESULTS

Processing of methods

Crown reconstructions from digital photographs using TA software were done following the procedure of Phattaralerphong and Sinoquet (2007). Data acquisition as reported by Phattaralerphong and Sinoquet (2007) was quick and software parameterization was not time-consuming. The two longest steps in the reconstruction were image processing (i.e. binarization), which may take several minutes for each image, and calculation time, which may take from 2 to 6 h, depending on the number of pictures and the size of the voxels chosen. In contrast, reconstruction from T-LiDAR scans required a long period of development, including the acquisition of field data measurements for the production of allometric relationships. Indeed, no tools based on this laser scanning approach are presently available in the literature, especially for deciduous trees. However, T-LiDAR data acquisition was simple and, once algorithms were developed, processing required about 8 h to reconstruct the crown and obtain its associated traits. If data acquisition for both methods faces the same limitations (mostly wind and occlusion), T-LiDAR has the substantial advantage over digital photography of being independent of background and contrast. However, the T-LiDAR approach represents a much more expensive investment (about US$150 000 for the instrument and software) compared with the digital photography (about US$1000).

Accuracy of trait extractions

With both methods, extraction of 2-D traits (H_t, L_t, H_c and $D_{c,mean}$) was acceptable, with respective mean deviations of

TABLE 1. *Comparison of measured and extracted 2-D and 3-D traits from digital photographs using* Tree Analyser *software with 7 cm (*TA-*7) or 3 cm (*TA-*3) voxel sizes, and from a reconstructed tree using terrestrial LiDAR scans (T-LiDAR)*

	Units	Measured	Extracted from TA-7	Extracted from TA-3	Extracted from T-LiDAR	TA-7 deviation (%)	TA-3 deviation (%)	T-LiDAR measured (%)
2-D traits								
H_t	m	2·02	2·13	2·11	2·01	5·4	4·5	(−) 0·5
L_t	m	2·05	2·13	2·11	2·04	3·9	2·9	(−) 0·4
H_c	m	1·89	2·05	1·98	1·93	8·5	4·8	2·1
$D_{c,mean}$	m	1·45	1·7	1·59	1·5	17·2	9·7	3·4
3-D traits								
V_c	m^3	0·69	1·73	1·10	0·59	150·7	59·4	(−) 14·5
A_c	m^2	1·88	2·32	2·19	1·77	31·1	23·7	(−) 5·9

Deviations from measured values are presented as percentages for each of the three methods.

8·8, 5·4 and 1·6 % for TA-7, TA-3 and T-LiDAR, respectively (Table 1). On 2-D traits, TA-7 thus showed an absolute error of about 15 cm, which was reduced to 10 cm when using smaller voxels of 3 cm. However, when reducing the size of the voxels, the gain in precision occurred mainly for H_c and $D_{c,mean}$, while deviations were not markedly reduced for H_t and L_t (Table 1). Moreover, the use of T-LiDAR scans greatly reduced the mean absolute error made on 2-D trait extractions to 2·8 cm. Most of this error was attributable to H_c and $D_{c,mean}$ (i.e. about 5 cm), while errors on H_t and L_t were about 1 cm and negative (i.e. led to an under-estimation).

Concerning 3-D traits, trait extraction was much less accurate, especially for crowns that had been reconstructed from digital photographs (cf. Fig. 1). First, TA-7 showed a deviation equivalent to 150·7 % of the measured V_c (Table 1). Secondly, reducing the size of the voxels to 3 cm reduced the deviation to 59·4 % of the measured V_c (Table 1). Thirdly, deviation of V_c estimated from T-LiDAR scans corresponded to 14·5 % of the measured V_c (Table 1). Reconstruction from T-LiDAR was thus reported as the most precise method to approach the actual volume occupied by all crown elements and, in contrast to TA reconstruction, T-LiDAR under-estimated V_c. Finally, extracted A_c values were more accurate than extracted V_c values. Deviations in A_c reached 31·1, 23·7 and 5·9 % for TA-7, TA-3 and T-LiDAR, respectively (Table 1). For T-LiDAR, the estimated A_c under-estimated the measured value, but the resulting absolute error was of about 0·11 m^2 (equivalent to 22 leaves of an average size).

TABLE 2. *Measured and extracted (from T-LiDAR) heights of branch insertion on the main stem*

Branch ID	Measured height of insertion (m)	Reconstructed height of insertion (m)	Deviation in height of insertion (%)	Absolute error in height of insertion (m)
1	0·08	0·08	0·0	0·00
2	0·1	0·08	−20·0	0·02
3	0·13	0·13	0·0	0·00
4	0·4	0·48	20·0	0·08
5	0·47	0·48	2·1	0·01
6	0·52	0·53	1·9	0·01
7	0·55	0·53	−3·6	0·02
8	0·59	0·58	−1·7	0·01
9	0·63	0·63	0·0	0·00
10	0·67	ND		
11	0·72	0·73	1·4	0·01
12	0·77	0·78	1·3	0·01
13	0·82	0·83	1·2	0·01
14	0·87	0·83	−4·6	0·04
15	0·93	0·83	−10·8	0·10
16	0·98	0·88	−10·2	0·10
17	1·02	0·98	−3·9	0·04
18	1·05	0·98	−6·7	0·07
19	1·07	1·08	0·9	0·01
Mean			1·8	0·03

Deviation (%) from the measured height and absolute error (m) are indicated for each branch.
ND, not detected.

Validation of crown reconstruction from T-LiDAR scans

To test specifically the reconstruction obtained from T-LiDAR associated with allometric relationships, four levels of validation were performed. First, the number of reconstructed branches ($n = 18$) was compared with the actual number of branches ($n = 19$). Reconstruction from T-LiDAR thus allowed detection and recreation of 95 % of the total main branches. Secondly, the heights of the main branch insertions (H_b) for reconstructed branches were compared with their measured heights (Table 2). Deviations of H_b ranged from 0 to 20 %, and the equivalent absolute error varied from 0 to 10 cm; for the majority of branches ($n = 14$), the error was kept under 5 cm (Table 2). Mean deviation and mean absolute error on H_b thus reached 1·8 % and 3 cm, respectively (Table 2). The third level of validation concerned the length of main branches (L_b) (Table 3). In this case, deviations and errors were much higher, varying from 0·2 to 66·4 % and from 0 to 35 cm, respectively (Table 3). Interestingly, the highest errors were reported for shorter branches located in the middle of the crown (Table 3). Finally, the last level of validation compared the reconstructed vertical profile of biomass distribution with the vertical profile of biomass calculated from the leaves-on T-LiDAR scans (Fig. 5). This comparison showed that biomass localization was satisfactory, especially below a height of 1·5 m (Fig. 5). For example, maximum biomass proportion was measured at a height of 60 cm in the actual profile, whereas maximum biomass proportion was found at

a height of 65 cm in the reconstructed profile. However, reconstruction failed to locate a significant portion of the biomass between heights of 75 and 80 cm and in the upper parts of the canopy, as compared with the profile measured from the leaf-on scene (Fig. 5B).

TABLE 3. *Measured and extracted (from T-LiDAR) length of branches*

Branch ID	Measured branch length (m)	Reconstructed branch length (m)	Deviation in branch length (%)	Absolute error in branch length (m)
1	1·74	1·70	−2·5	0·04
2	0·86	0·87	1·1	0·01
3	1·00	0·67	−33·3	0·33
4	0·23	0·13	−43·8	0·16
5	0·36	0·29	−20·0	0·08
6	0·39	0·23	−40·9	0·20
7	0·50	0·17	−66·4	0·34
8	0·51	0·21	−58·6	0·35
9	0·59	0·49	−17·7	0·13
10	0·73	ND		
11	0·59	0·34	−42·9	0·25
12	0·86	0·80	−6·5	0·06
13	0·83	0·69	−17·2	0·14
14	0·84	0·84	0·2	0·00
15	0·96	0·84	−12·4	0·12
16	0·79	0·63	−20·8	0·16
17	0·9	0·71	−20·9	0·19
18	1·09	1·07	−2·2	0·02
19	1·11	1·06	−4·2	0·05
Mean			−22·8	0·15

Deviation (%) from the measured length and absolute error (m) are indicated for each branch.

ND, not detected.

DISCUSSION

Method processing and development

As a first objective, our aimwas to develop a rapid and accurate method for crown reconstruction using T-LiDAR scans. Such an approach is thought to be particularly promising and is presently under development by a number of research groups (Côté *et al.*, 2009; Livny *et al.*, 2010; Preuksakarn *et al.*, 2010). The theoretical approaches to the reconstruction of tree crowns from T-LiDAR scans are numerous and generally differ due to size, shape and species of targeted trees. Here, we chose to combine a minimum spanning tree approach with modelling to reconstruct the whole crown. Indeed, T-LiDAR technology has the ability to capture the 3-D organization of elements in space, but occlusion and wind generally hinder precise reconstruction out to the branch tips or leaves. For large conifers, Côté *et al.* (2009) settled on the partitioning between stem and foliage points within the point cloud. Stem points were used for algorithm-driven reconstruction, while foliage points were used as attractors for a modelled reconstruction. For deciduous trees, we argue that using modelling to locate leaves on a precise skeleton built from T-LiDAR scans of leaf-off scenes will allow a better reconstruction than reconstructions only from leaf-on scenes. Indeed, broad leaves represent an important source of occlusion that interferes with detecting branch tips and other leaves. Furthermore, two arguments reinforced this 'leaf-off' approach: (1) the important developments currently occurring with regards to skeleton reconstruction methods from 3-D point clouds or 3-D surfaces (Dey and Sun, 2006; Reniers and Telea, 2007; Runions *et al.*, 2007; Bucksch and Lindenbergh, 2008; Yan *et al.*, 2009; Bucksch *et al.*, 2010); and (2) the high quality scans that can be acquired for deciduous species during leaf-off periods such as autumn and

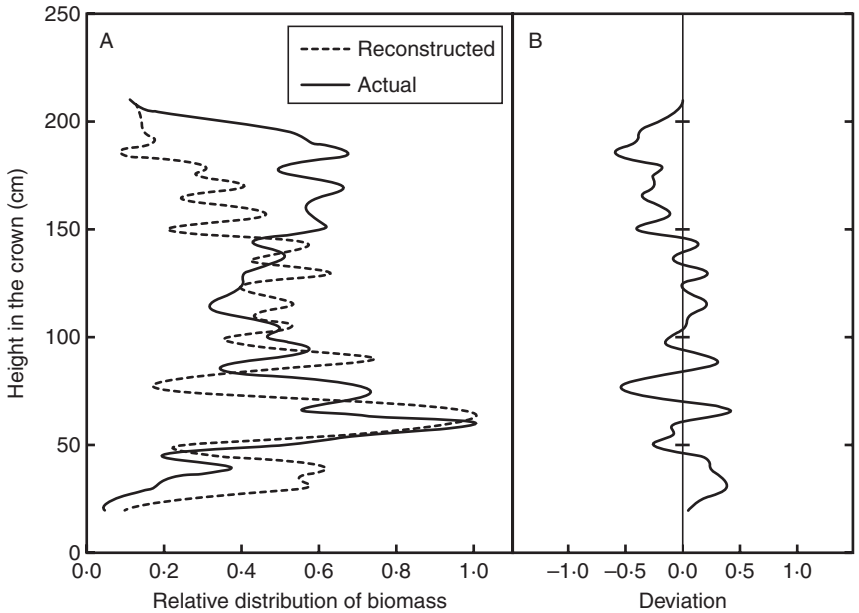

FIG. 5. (A) Representation of actual (from T-LiDAR leaf-on scene) and reconstructed (from T-LiDAR leaf-off scene and modelling) vertical profiles of object distribution within the crown of the studied poplar sapling. (B) Illustration of the deviation between actual and reconstructed vertical profiles of biomass. Negative and positive values refer to under- and over-estimation of the reconstruction.

spring (Bucksch and Fleck, 2009). Consequently, we designed a simple algorithm inspired by the approach of Verroust and Lazarus (1997) to reconstruct the tree skeleton. On this framework, leaves were added using simple allometric relationships (see Casella and Sinoquet, 2003). Similar approaches that add foliage to a reconstructed skeleton have already been used by Xu *et al.* (2007) for deciduous trees and by Côté *et al.* (2009) for large coniferous trees. In the present study, both components of the reconstruction (i.e. skeletization and modelling) were very simple and robust, but new allometric relationships have to be established when reconstructing the crown of another species or clone.

With regard to TA, this tool was developed by Phattaralerphong and Sinoquet (2005, 2007) and is based on space carving theory (Martin and Aggarwal, 1983) for volume and surface estimation. This method is efficient and might be of interest due its low cost and mobility. However, few developments have occurred in stereophotogrammetry for forest applications in the last few years. Indeed, significant developments based on digital image processing have only arisen in movie post-production, architectural designs and video games (Seitz *et al.*, 2006; Neubert *et al.* 2007; Tan *et al.*, 2008).

Accuracy of the methods for trait extraction and validation of T-LiDAR reconstruction

Both methods were suitable for extraction of 2-D traits. This was expected for TA, since Phattaralerphong and Sinoquet (2005) have already reported on the accuracy of this method for extracting such dimensions on trees of several species and sizes. However, we recorded a slightly larger error than that reported by Phattaralerphong and Sinoquet (2005), an error which may arise from three contrasting sources. First, the voxel approach obviously enlarged the reconstructed crown, leading to over-estimation associated with the selected size of the voxel; the larger the voxel, the greater the over-estimation. Secondly, TA algorithms consider that all voxels contain foliage. This may over-estimate volume, especially for canopies with low leaf density. Finally, error may have increased in our more operational context due to our ability to measure camera distance from the target as well as camera angles. Indeed, these field constraints may have led to slight cumulative offsets when combining all photographs. One important result also concerned the accuracy of extractions of 2-D traits using the T-LiDAR reconstruction. This accuracy is associated with the ability of LiDAR scans to obtain valuable information on an object's silhouette, where occlusion is minimized.

With regard to 3-D traits, a greater discrepancy was found between the two methods with regard to accuracy. As with 2-D traits, errors of TA in these extractions increased due to the voxel approach and to the field measurements that were required to determine the relative position of the camera. For these traits, an additional source of error corresponded to the three viewpoints that were used here for space carving compared with the eight used by Phattaralerphong and Sinoquet (2005). Reducing the number of viewpoints obviously increased the number of voxels retained during space carving, leading to over-estimation. However, the parameterization needed in TA to estimate A_c from V_c (i.e. basically, a quantification of foliage density) largely corrected for the over-estimation reported in V_c (cf. Table 1). Having good estimates of foliage density and organization in space, mainly through $A_{l,mean}$ and $\theta_{l,mean}$, is sufficient to obtain a plausible estimate of A_c. Unfortunately, this estimated area is not spatially explicit, which greatly limits the use of such a trait. In parallel, 3-D traits estimated from T-LiDAR reconstruction showed lower deviations from empirical measurements. However, both A_c and V_c were under-estimated, leading us to conclude that information was lost during the reconstruction process. For A_c, our validation exercise showed that one medium-sized branch in the middle of the crown was missed by the reconstruction algorithm. This loss of information is attributable to a combination of factors. First, the inner position of the branch within the crown may have led to partial occlusion in this part of the registered scan. This interpretation is reinforced by the fact that error on branch length was generally higher on smaller and lower branches, which are not clearly emerging from the crown volume (Table 3). These branches were defined, therefore, by a lower number of points and by more isolated points, which in turn may be more easily removed during scan filtering. Another critical concern related to the algorithm we elaborated is the angle of branch insertion. Since we used horizontal layers to define centroids, very horizontal branches, with most of their biomass contained in a single layer, may be severely under-estimated. Finally, validation of the vertical profile of biomass within the crown showed that allometric relationships used for foliage reconstruction slightly under-estimated A_l in the upper ($>1{\cdot}5$m) part of the crown, where larger leaves are located, compared with the lower portion of the crown. Nevertheless, despite these observed deviations, final reconstruction from T-LiDAR using the colonization algorithm and allometric relationships produced a deviation $<6\,\%$, which was equivalent to about 22 leaves of an average size (cf. Fig. 4A).

Versatility of the methods

Both the T-LiDAR and digital photography methods were tested in a more operational context (only three clear viewpoints) to assess their ability to extract accurate 2-D and 3-D traits. For its cost, TA showed very interesting results for 2-D traits, and it would be preferred on isolated trees since: (*a*) only H_t, H_c and $D_{c,mean}$ are targeted; and (*b*) the background can be controlled to some extent. For example, this method may be used to survey height, crown expansion and yields in plantation systems. However, no more information can obviously be extracted from these TA reconstructions, and linkages with FSPM or any dynamic modelling exercises are extremely limited. In the future, developments in tree crown reconstructions from digital images may thus depend on other approaches (Mizoue and Masutani, 2003; Neubert *et al.*, 2007; Tan *et al.*, 2008). In contrast, T-LiDAR appeared to be very efficient in estimating both 3-D and 2-D traits. Most importantly, 3-D traits extracted using this method, such as A_c and its profile, are spatially explicit and can be coupled to phylloclimate models (Chelle, 2005) to survey individual environmental conditions or can even be used to integrate whole tree photosynthetic production (Adam *et al.*, 2006).

Moreover, the instantaneous picture obtained of the real tree from T-LiDAR scans can be used to feed FSPM [e.g. LIGNUM (Perttunen *et al.*, 1998), YPLANT (Pearcy and Yang, 1996) and GREENLAB (de Reffye *et al.*, 1997)] to predict future individual development over longer time periods.

Conclusions

Taking into account their cost, the magnitude of their data acquisition and analysis, and their accuracy for trait estimations, digital images or T-LiDAR scans are valuable technologies to extract information from trees in an operational context. However, both methods offer very contrasting services in terms of reconstruction. Rapid surveys of isolated trees may be achieved using TA, but not much more can presently be extracted using such a tool. In contrast, T-LiDAR is a particularly promising tool for investigating the structure and development of large perennial deciduous plants. Indeed, despite a rather substantial investment in time for the initial parameterization of trait extractions, continuous development of algorithms greatly expands the number of traits which can be extracted and constantly simplifies their extraction. Ultimately, linkages between T-LiDAR-based remote sensing and FSPM may increase opportunities for tree modelling and study.

ACKNOWLEDGEMENTS

We are grateful to Richard Fournier (University of Sherbrooke) for the invaluable loan of the scanning device and his comments concerning the development of the crown reconstruction method from T-LiDAR scans. We also acknowledge Myriam Lemelin and Emilie Lessard for their help in performing the scans, harvesting the leaves and collecting validation data, and William F. J. Parsons for English language editing. This study was supported by a Discovery Grant (to S.D.) from the Natural Sciences and Engineering Research Council (NSERC) of Canada.

LITERATURE CITED

Adam B, Dones N, Sinoquet H. 2006. *VegeSTAR3·2·4 calcul de l'interception lumineuse et de la photosynthèse*. INRA-PIAF: Clermont Ferrand, France.

Bucksch A, Fleck S. 2009. Automated detection of branch dimensions in woody skeletons of leafless fruit. *SilviLaser 2009 proceedings*, 14–16 October 2009 Austin, Texas.

Bucksch A, Lindenbergh R. 2008. CAMPINO – a skeletonization method for point cloud processing. *ISPRS Journal of Photogrammetry and Remote Sensing* **63**: 115–127.

Bucksch A, Lindenbergh R, Menenti M, Raman M. 2009. Skeleton-based botanic tree diameter estimation from dense LiDAR data. In: Singh UN. ed. *Lidar Remote Sensing for Environmental Monitoring, Proceedings of SPIE*, vol. 7460.

Bucksch A, Lindenbergh R, Menenti M. 2010. SkelTre: robust skeleton extraction from imperfect point clouds. *The Visual Computer* **26**: 1283–1300.

Casella E, Sinoquet H. 2003. A method for describing the canopy architecture of coppice poplar with allometric relationships. *Tree Physiology* **23**: 1153–1169.

Chambelland J, Dassot M, Adam B, *et al*. 2008. A double-digitising method for building 3D virtual trees with non-planar leaves: application to the morphology and light-capture properties of young beech trees (*Fagus sylvatica*). *Functional Plant Biology* **35**: 1059–1069.

Chelle M. 2005. Phylloclimate or the climate perceived by individual plant organs: What is it? How to model it? What for? *New Phytologist* **166**: 781–790.

Côté J-F. 2010. *Modélisation de l'architecture des forets pour améliorer la télédétection des attributs forestiers*. PhD dissertation, Université de Sherbrooke (Qc), Canada. 2010. Publication No. AAT NR6422. Available from: http://www.proquest.com/.

Côté J-F, Widlowski J-L, Fournier R, Verstraete MM. 2009. The structural and radiative consistency of three-dimensional tree reconstructions from terrestrial lidar. *Remote Sensing of Environment* **113**: 1067–1081.

Delagrange S, Montpied P, Dreyer E, Messier C, Sinoquet H. 2006. Does shade improve light interception efficiency? A comparison among seedlings from shade-tolerant and -intolerant temperate deciduous tree species. *New Phytologist* **172**: 293–304.

Dey T, Sun J. 2006. Defining and computing curve skeletons with medial geodesic function. *Proceedings of the Symposiumo on Geometry Processing*, 143–152.

Di Iorio A, Laserre B, Scippa G, Chiatante D. 2005. Root system architecture of *Quercus pubescens* trees growing on different sloping conditions. *Annals of Botany* **95**: 351–361.

Doyon F, Nolet P, Forget E, Pouliot R. 2006. COHORTE: a distance-independent individual tree model to assess stand growth and quality grade changes under partial cutting regimes. *Conference Proceedings: IUFRO 1·05 conference on Natural disturbance-based silviculture – Managing for complexity*, Rouyn-Noranda, Québec, Canada, 194.

Farque L, Sinoquet H, Colin F. 2001. Canopy structure and light interception in *Quercus petraea* seedlings in relation to light regime and plant density. *Tree Physiology* **21**: 1257–1267.

Hosoi F, Omasa K. 2006. Voxel-based 3-D modeling of individual trees for estimating leaf area density using high-resolution portable scanning LiDAR. *IEEE Transactions on Geoscience and Remote Sensing* **44**: 3610–3618.

Houllier F, de Reffye P. 2006. Linking tree architecture, stem growth and timber quality: a review of some modelling approaches. *Proceedings of the second workshop: Connection between silviculture and wood quality through modelling approaches and simulation softwares*, 26–31 August 2006, Berg en Dal, South Africa, 294–303.

Lambert MC, Ung CH, Raulier F. 2005. Canadian national tree aboveground biomass equations. *Canadian Journal of Forest Research* **35**: 1996–2018.

Livny Y, Yan F, Olson M, Chen B, Zhang H, El J. 2010. Automatic reconstruction of tree skeletal structures from point clouds. *ACM Transactions on Graphics* **29**: Art.151 8p.

Martin WN, Aggarwal JK. 1983. Volumetric descriptions of objects from multiple views. *IEEE Transactions on Pattern Analysis and Machine Intelligence* **PAMI-5**: 150–158.

Mizoue N, Masutani T. 2003. Image analysis measure of crown condition, foliage biomass and stem growth relationships of *Chamaecyparis obtusa*. *Forest Ecology and Management* **172**: 79–88.

Neubert B, Franken T, Deussen O. 2007. Approximate image-based tree-modeling using particle flows. *ACM Transactions on Graphics* **26**: Article 88. doi:10.1145/1276377.1276487.

Pacala SW, Canham CD, Silander JA. 1993. Forest models defined by field measurements: I. The design of a northern forest simulator. *Canadian Journal of Forest Research* **23**: 1980–1988.

Pearcy RW, Yang W. 1996. A three-dimensional crown architecture model for assessment of light capture and carbon gain by understory plants. *Oecologia* **108**: 1–12.

Pearcy RW, Muraoka H, Valladares F. 2005. Crown architecture in sun and shade environments: assessing function and trade-offs with a three-dimensional simulation model. *New Phytologist* **166**: 791–800.

Perttunen J, Sievänen R, Nikinmaa E. 1998. LIGNUM: a model combining the structure and the functioning of trees. *Ecological Modelling* **108**: 189–198.

Perttunen J, Nikinmaa E, Lechowicz MJ, Sievanen R, Messier C. 2001. Application of the functional–structural tree model LIGNUM to sugar maple saplings (*Acer saccharum* Marsh) growing in forest gaps. *Annals of Botany* **88**: 471–481.

Phattaralerphong J, Sinoquet H. 2005. A method for 3D reconstruction of tree crown volume from photographs: assessment with 3D-digitized plants. *Tree Physiology* **25**: 1229–1242.

Phattaralerphong J, Sinoquet H. 2007. *Tree analyser: software to compute tree structure parameters from photographs*. User manual. PIAF-INRA. http://www2.clermont.inra.fr/piaf/eng/download/download.php.

Preuksakarn C, Boudon F, Ferraro P, Durand J-B, Nikinmaa E, Godin C. 2010. Reconstructing plant architecture from 3D laser scanner data. In: DeJong T, Da Silva D. eds. *Proceedings of the 6th International Workshop on Functional–Structural Plant Models*, 12–17 September 2010, Davis, CA, USA, 14–16.

Prusinkiewicz P, Karwowski R, Lane B. 2007. The L + C plant-modelling language. In: Vos J, *et al*. eds. *Functional–structural plant modelling in crop production*. Berlin: Springer, 27–42.

Reniers D, Telea A. 2007. Skeleton-based hierarchical shape segmentation. In: Galin E, Wyvill B, Pauly M. eds. *Proceedings of the IEEE International Conference on Shape Modeling and Applications*, 13–15 June 2007, Lyon, France. Los Alamitos, CA: IEEE Computer Society, 179–188.

de Reffye P, Fourcaud T, Blaise F, Barthélémy D, Houllier F. 1997. A functional model of tree growth and tree architecture. *Sylva Fennica* **31**: 297–311.

Rosell JR, Llorens J, Sanz R, *et al*. 2009. Obtaining the three-dimensional structure of tree orchards from remote 2D terrestrial LIDAR scanning. *Agricultural and Forest Meteorology* **149**: 1505–1515.

Runions A, Lane B, Prusinkiewicz P. 2007. Modeling trees with a space colonization algorithm. In: Ebert D, Mérillou S. eds. *Proceeding of Eurographics Workshop on Natural Phenomena*, 1 April, 2007, Munich, Germany. Eurographics Association, 63–70.

Seitz S, Curless B, Diebel J, Scharstein D, Szeliski R. 2006. A comparison and evaluation of multi-view stereo reconstruction algorithms. In: Fitzgibbon A, Taylor CJ, LeCun Y. eds. *Proceedings of the 2006 IEEE Computer Society Conference on Computer Vision and Pattern Recognition*. Washington, DC: IEEE Computer Society, 519–529.

Shlyakhter I, Rozenoer M, Dorsey J, Teller S. 2001. Reconstructing 3D tree models from instrumented photographs. *IEEE Computer Graphics and Applications* **21**: 53–61.

Sinoquet H, Thanisawanyangkura S, Mabrouk H, Kasemsap P. 1998. Characterization of the light environment in canopies using 3D digitising and image processing. *Annals of Botany* **82**: 203–212.

Sonohat G, Sinoquet H, Kulandaivelu V, Combes D, Lescourret F. 2006. Three-dimensional reconstruction of partially 3D-digitized peach tree canopies. *Tree Physiology* **26**: 337–351.

Tan P, Fang T, Xiao J, Zhao P, Quan L. 2008. Single image tree modeling. *ACM Transactions on Graphics* **27**: Article 108. doi:10.1145/1409060.1409061.

Verroust A, Lazarus F. 1997. Extracting skeletal curves from 3d scattered data. *The Visual Computer* **16**: 15–25.

Xu H, Gossett N, Chen B. 2007. Knowledge and heuristic-based modeling of laser-scanned trees. *ACM Transactions on Graphics* **26**: Article 19. doi:10.1145/1289603.1289610.

Yan DM, Wintz J, Mourrain B, Wang W, Boudon F, Godin C. 2009. Efficient and robust reconstruction of botanical branching structure from laser scanned points. In: Thalman D, Shah JJ, Peng Q. eds. *11th IEEE International conference on Computer-Aided Design and Computer Graphics (CAD/Graphics 2009)*. IEEE Press, 572–575.

APPENDIX

Abbreviations, description and units of the parameters used in both reconstruction methods

Abbreviation	Units	Description
$A_{l,mean}$	cm^2	Mean leaf area
$\theta_{L,mean}$	°	Mean leaf elevation angle in the whole crown
$D_{i,\ j,mean}$	m	Mean of all distances of x, y, z points from the centroid j in the layer i. It becomes the radious of the pipe object in the layer i in the reconstruction
N_l	Number	Number of leaf
$L_{l,max}$	m	Maximal leaf length
L_s	m	Current-year shoot length
L_b	m	Branch length
A_L	m^2	Area of a leaf
L_l	m	Leaf length
$L_{rel.pos.}$	–	Relative position of the leaf on the current-year shoot
β	–	Coefficient for the reduction of maximal leaf length
Φ_l	°	Leaf rolling angle
θ_l	°	Leaf elevation angle
Ψ_l	°	Leaf azimuth angle
H_t	m	Total tree height (vertical distance)
L_t	m	Total length of the tree (along the stem)
H_c	m	Crown height (i.e. vertical distance between the lower and upper point of the crown)
D_c	m	Crown diameter
$D_{c,mean}$	m	Mean crown diameter (average of the diameter in four directions)
H_b	m	Height of the branch insertion on the main stem
A_c	m^2	Total leaf area of the whole crown
V_c	m^3	Volume of the whole crown